ISEIS

Journal of Environmental Informatics 15(1) 26-32 (2010)

Journal of Environmental Informatics

www.iseis.org/jei

Modeling Acoustic Properties of the Fluid-Fluid Interface in Porous Medium

N. Y. Liu[1], R. Paranjape[1,*], and K. Asghari[2]

[1]*Electronic Systems Engineering, University of Regina, Regina, Saskathewan S4S 0A2, Canada*
[2]*Petroleum Systems Engineering, University of Regina, Regina, Saskathewan S4S 0A2, Canada*

Received 29 August 2008; revised 17 September 2009; accepted 11 October 2008; published online 10 March 2010

ABSTRACT. The purpose of this study is to present mathematical modeling of the acoustic properties of fluid-fluid interface in porous medium in order to to identify fluid-fluid interfaces according to their different acoustic properties. Biot's theory of acoustic wave's propagation in homogenous porous medium is used to calculate reflection and transmission coefficients of an interface in the porous medium. It is found that these coefficients are sensitive to the frequency and the angle of the incident wave, which is regarded as the significant acoustic property of fluid-fluid interfaces and of discontinuities of the porous medium. Acoustic properties of general fluid-fluid interfaces or porous medium discontinuities are presented as series of plots of coefficient magnitude versus incident frequency or angle. It is shown that there is significant acoustic difference between a fluid-fluid interface and a discontinuity of the porous medium, which can be used to identify a fluid-fluid interface. Here, methods are designed to locate, identify a fluid-fluid interface, and measure its shape, using reflection and/or transmission of waves.

Keywords: sonar probing, modeling acoustic properties of interfaces, Biot's theory, computer simulation

1. Introduction

One potential technique for investigating the location and shape of the fluid-fluid interface in porous media is through acoustic probing. This technique can be utilized for monitoring various processes involving fluid displacement in porous media, such as those observed during carbon dioxide (CO_2) flooding of oil reservoirs. In this proposed method, acoustic transducers emit acoustic waves towards the fluid-fluid interface; while other transducers receive the reflected and transmitted acoustic energy.

Proper analysis of these transmitted and reflected signals can be used to determine the location and shape of the fluid-fluid interface and to distinguish it from other discontinuities found in porous media, such as presence of faults and variations in spatial permeability. .

One of the applications of such technique can be during CO_2 flooding operations, where CO_2 is injected into oil fields for improving oil recovery and for the purpose of geological storage of CO_2. Injection of CO_2 in petroleum producing reservoirs has been accepted as a viable approach to reduce emissions of green house gases, such as CO_2, into atmosphere. Figure 1 presents a schematic of carbon dioxide flooding process in oil reservoirs. Here, carbon dioxide is injected from injection wells into the reservoir, where it comes into contact with oil in the reservoir and mobilizes the oil towards production wells. In the reservoir, an interface between injected CO_2 and oil gets established. This interface separates CO_2-rich part of reservoir from oil-rich region and moves from injection wells towards production wells. It is of great importance to know the location and the shape of this fluid-fluid interface in order to better control, monitor, and manage the CO_2 flood.

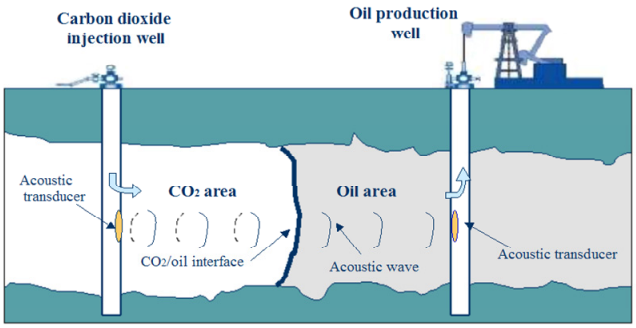

Figure 1. CO_2-flood for sequestration and enhanced oil recovery (EOR).

Currently there are few techniques proposed for monitoring CO_2 in porous geological formations. Four-dimensional (4D) (time-lapse), three-component (3C) (multi-component) seismic is the most advanced technique used for this purpose (Benson and Davis, 2000). The newly developed time-lapse seismology can be used for determining reservoir property variations under changing conditions. This is an effective method, but it is very

* Corresponding author. Tel.: +1 306 5855290; fax: +1 306 5854855.
E-mail address: raman.paranjape@uregina.ca (R. Paranjape).

ISSN: 1726-2135 print/1684-8799 online
 doi:10.3808/jei.201000163

costly to implement and time consuming. Another method proposed for monitoring CO_2 in oil reservoirs is based on a technique that has been developed initially for gas flooding. This method is based on utilizing neutron logs for computing two porosities: the base true porosity determined before injecting CO_2 and monitor-apparent neutron porosity determined after CO_2 injection (Ruhovets, 1995). Another process proposed for monitoring movement of CO_2 in oil reservoirs is by injecting and monitoring radioactive isotopes of CO_2 (Juprasert et al., 1999). This method can provide general information about volumetric sweep efficiency of CO_2, but the information obtained from this method cannot be used for monitoring the shape and location of the CO_2-oil interface.

It is the objective of this paper to present a novel approach for utilizing acoustic waves for monitoring the shape and location of this interface. A theoretical analysis of suitability of acoustic waves for this purpose is presented in this paper.

Here, a careful analysis and modeling of the propagation of acoustic waves in porous media containing two different fluids is presented, where Biot's theory has been utilized to describe wave propagation in a porous media containing CO_2 and oil.

2. Biot's theory

The mathematical representation of Biot's theory of wave propagating in saturated porous media is presented as a system of equations below (Biot, 1956, 1962a, b; Berryman, 1980; Bourbie et al., 1987):

$$\nabla\cdot\tau = H_c\nabla(\nabla\cdot U) - \mu\nabla\times(\nabla\times U) + D\nabla(\nabla\cdot W) = \rho\frac{\partial^2 U}{\partial t^2} + \rho_f\frac{\partial^2 W}{\partial t^2} \quad (1a)$$

$$-\nabla p = D\nabla(\nabla\cdot U) + M\nabla(\nabla\cdot W) = \rho_f\frac{\partial^2 U}{\partial t^2} + g\frac{\partial^2 W}{\partial t^2} + b\frac{\partial W}{\partial t} \quad (1b)$$

Definition of various variables in Equations (1a) and (1b) is presented in the abbreviation section at the end of this paper. Above set of equations have been utilized for describing the propagation and reflection of waves in porous media saturated by two different fluids as follows.

2.1. Model of Reflection and Transmission of a Wave at an Interface

According to various studies when an incident wave encounters an interface, which can be a fluid-fluid interface in porous medium or a parameter discontinuity of porous medium itself, six types of waves will be generated (Santos et al., 1992; Wu et al., 1990; Deresiewicz, 1960; Deresiewicz and Rice, 1962, 1964; Albert, 1993). These are reflected compressional type I waves, compressional type II waves, shear waves, transmitted compressional type I waves and compressional type II waves, and their corresponding shear waves. Figure 2 shows a shematic of reflection and transmission of an incident wave at an interface.

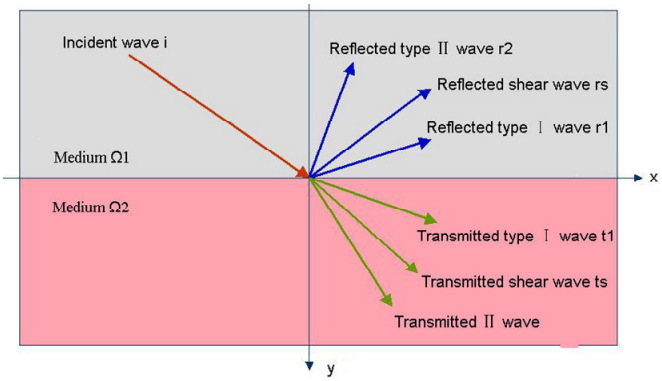

Figure 2. Reflection and transmission model of acoustic waves in porous media.

For each type of wave generated, there is a propagating coefficient "q", which describes the waves velocity and attenuation coefficient in a the form of a complex number. The complex wave vector q of a compressional wave satisfies Equation 2, where j is the imaginary unit:

$$(MH_c - D^2)q^4 + [\omega^2(2\rho_f D - gH_c - \rho M) + j\omega bH_c]q^2 + \omega^4(\rho g - \rho_f^2) - j\omega^3\rho b = 0 \quad (2)$$

Solution of the above equation provides two physical meaningful roots of q_1 and q_2, as well as two negative imaginary part corresponding to the type I and type II compressional waves, respectively.

Similarly, the complex wave vector q of a shear wave satisfies the equation below:

$$q^2 = \frac{\omega^2}{\mu}(\rho - \frac{\rho_f^2}{g - jb/\omega}) \quad (3)$$

The physical meaningful root q_s also has a negative imaginary part. If θ is defined as the angle of a wave and the y axis, then:

$$\alpha = q\sin\theta \quad (4a)$$

$$\beta = q\cos\theta \quad (4b)$$

According to Snell's law, we have:

$$\alpha_{r1} = \alpha_{r2} = \alpha_{rs} = \alpha_{t1} = \alpha_{t2} = \alpha_{ts} = \alpha_i \quad (5)$$

Different subscripts indicate various types of waves as shown in Figure 2. Furthermore, the reflection and transmission angles can be calculated as:

$$\theta_{mn} = \arcsin(q_i\sin\theta_i/q_{mn}),\ m = r, t;\ n = 1, 2, s \quad (6)$$

It worth mentioning that above equations and derivations

are based on research reported by Wu *et al*. (1990). The characteristics of the porous medium and the fluids on both sides of the fluid interface determine the relationship among these angles. Figure 3 shows a representative example of how the reflection and transmission angles vary as a function of the incident angle.

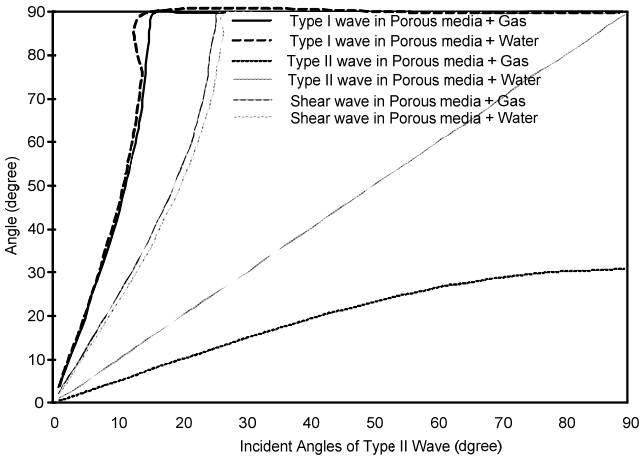

Figure 3. Reflection and transmission angles vary with the incident angle.

3. Identifation of the Fluid-fluid Interface

Acoustic reflections and transmissions are affected by physical discontinuities in the porous medium, as well as the fluid-fluid interfaces. Therefore, it is important to be able to distinguish porous media discontinuities from a genuine fluid-fluid interface. In this part, it has been demonstrated that the acoustic characteristics of a fluid-fluid interface are different from those of a porous medium discontinuity. Hence, acoustic waves can be utilized for identifying the fluid-fluid interface in reservoirs regardless of the presence of heterogeneities in the porous media.

3.1. Calculation of reflection and transmission coefficients at a linear interface

Let us consider a plane interface, Γ, at $z = 0$, which separates two regions of fluid-saturated porous media, Ω_1 and Ω_2 (as seen in Figure 2). The boundary conditions at the interface Γ are:

$$U_x^{(1)} = U_x^{(2)} \tag{7a}$$

$$U_z^{(1)} = U_z^{(2)} \tag{7b}$$

$$\tau_{zz}^{(1)} = \tau_{zz}^{(2)} \tag{7c}$$

$$\tau_{xz}^{(1)} = \tau_{xz}^{(2)} \tag{7d}$$

$$p^{(1)} = p^{(2)} \tag{7e}$$

$$W_z^{(1)} = W_z^{(2)} \tag{7f}$$

From the boundary conditions above, the reflection and transmission coefficients are calculated as (Wu et al., 1990):

$$C = F_i/R \tag{8}$$

C is defined as reflection and transmission coefficient vector $[E_{r1}, E_{r2}, E_{rs}, E_{t1}, E_{t2}, E_{ts}]$. R is given by:

$$R = \begin{bmatrix} \alpha_{r1} & \alpha_{r2} & \beta_{rs} & -\alpha_{t1} & -\alpha_{t2} & -\beta_{ts} \\ \beta_{r1} & \beta_{r2} & -\alpha_{rs} & -\beta_{t1} & -\beta_{t2} & \alpha_{ts} \\ \sigma_{r1} & \sigma_{r2} & -\sigma_{rs} & -\sigma_{t1} & -\sigma_{t2} & \sigma_{ts} \\ \alpha_{r1}\beta_{r1}\mu^{(1)} & \alpha_{r2}\beta_{r2}\mu^{(1)} & (\beta_{rs}^2 - \alpha_{rs}^2)\mu^{(1)}/2 & -\alpha_{t1}\beta_{t1}\mu^{(2)} & -\alpha_{t2}\beta_{t2}\mu^{(2)} & -(\beta_{ts}^2 - \alpha_{ts}^2)\mu^{(2)}/2 \\ \delta_{r1} & \delta_{r1} & 0 & -\delta_{t1} & -\delta_{t2} & 0 \\ \beta_{r1}\gamma_{r1} & \beta_{r2}\gamma_{r2} & -\alpha_{rs}\gamma_{rs} & -\beta_{t1}\gamma_{t1} & -\beta_{t2}\gamma_{t2} & \alpha_{ts}\gamma_{ts} \end{bmatrix} \tag{9}$$

where γ_{mn}, σ_{mn} and δ_{mn} are given by:

$$\gamma_{rn} = (\rho^{(1)}\omega^2 - q_{rn}^2 H_c^{(1)})/(q_{rn}^2 D^{(1)} - \rho_f^{(1)}\omega^2)\ ,\ n = 1, 2 \tag{10a}$$

$$\gamma_{tn} = (\rho^{(2)}\omega^2 - q_{tn}^2 H_c^{(2)})/(q_{tn}^2 D^{(2)} - \rho_f^{(2)}\omega^2)\ ,\ n = 1, 2 \tag{10b}$$

$$\gamma_{rs} = (\mu^{(1)} q_{rs}^2 - \rho^{(1)}\omega^2)/\rho_f^{(1)}\omega^2 \tag{10c}$$

$$\gamma_{ts} = (\mu^{(2)} q_{ts}^2 - \rho^{(2)}\omega^2)/\rho_f^{(2)}\omega^2 \tag{10d}$$

$$\sigma_{rn} = -H_c^{(1)} q_{rn}^2 - D^{(1)} q_{rn}^2 \gamma_{rn} + 2\mu^{(1)}\alpha_{rn}^2\ ,\ n = 1, 2 \tag{10e}$$

$$\sigma_{tn} = -H_c^{(2)} q_{tn}^2 - D^{(2)} q_{tn}^2 \gamma_{tn} + 2\mu^{(2)}\alpha_{tn}^2\ ,\ n = 1, 2 \tag{10f}$$

$$\delta_{rn} = (D^{(1)} + M^{(1)}\gamma_{rn}) q_{rn}^2\ ,\ n = 1, 2 \tag{10g}$$

$$\delta_{tn} = (D^{(2)} + M^{(2)}\gamma_{tn}) q_{tn}^2\ ,\ n = 1, 2 \tag{10h}$$

$$\sigma_{rs} = 2\mu^{(1)}\alpha_{rs}\beta_{rs} \tag{10i}$$

$$\sigma_{ts} = 2\mu^{(2)}\alpha_{ts}\beta_{ts} \tag{10k}$$

where β_{rn} ($n = 1, 2, s$) are obtained from $\beta_{rn}^2 = q_{rn}^2 - \alpha_{rn}^2$ and real(β_{rn}) <0; β_{tn} ($n = 1, 2, s$) are obtained from $\beta_{tn}^2 = q_{tn}^2 - \alpha_{tn}^2$, and real($\beta_{tn}$) < 0. If a compressional wave is the incident wave,

$$F_i = [-\alpha_i, -\beta_i, -\sigma_i, -\alpha_i\beta_i\mu^{(1)}, -\delta_i, -\beta_i\gamma_i]^T. \quad (11a)$$

If a shear wave is the incident wave,

$$F_i = [-\beta_i, \alpha_i, \sigma_i, -(\beta_i^2 - \alpha_i^2)\mu^{(1)}/2, 0, -\alpha_i\gamma_i]^T. \quad (11b)$$

In Equations (11a) and (11b), $\sigma_i = \sigma_{rn}$, $\delta_i = \delta_{rn}$, $\gamma_i = \gamma_{rn}$, in which n is determined by the type of the incident wave.

3.2. Investigating the Discontinuity of porous media with an incident shear wave

From Equation (3) of a complex wave vector of a shear wave, it is observed that q_s is only related to parameter S, φ, k of the porous medium. Equations (10c) to (10k) indicate that $\alpha_{ms}, \beta_{ms}, \gamma_{ms}, \sigma_{ms}$ ($m = r, t$) are also independent of the parameters of the porous medium except for S, φ, k.

If we assume the porous medium coefficients S, φ, k of Ω_1 are equal to those of Ω_2, as well as the fluid in Ω_1 and Ω_2 are the same q_{s1} of Ω_1 is always equal to q_{s2} of Ω_2. In this situation, if we apply a shear wave as the incident wave, we can observe the vector F_i is equal to column 6 of R. Under these conditions, the reflection and transmission coefficients will be:

$$C = F_i/R = [E_{r1}, E_{r2}, E_{rs}, E_{t1}, E_{t2}, E_{ts}] = [0, 0, 0, 0, 0, 1] \quad (12)$$

This result means that discontinuities of the porous medium do not affect the propagating of an incident shear wave, and no new reflection or transmission waves will be produced in this situation.

On the other hand, when a shear wave encounters a fluid-fluid interface, reflection and transmission waves are produced as modeled in Figure 2. It can be concluded that a shear wave as the incident wave can be used to discriminate fluid-fluid interfaces from discontinuities of the porous medium, such as variations in permeability or presence of faults.

3.3. Identification of the fluid-fluid interface using reflection and transmission coefficient at curve interface

It is found that the acoustic characteristics of a fluid-fluid interface and a discontinuity of porous medium are acoustically different. This difference is observed from amplitude vs. frequency or amplitude vs. incident-angle plots shown in Figures 4 and 5. In Figure 4, the porous medium is homogeneous in Ω_1 and Ω_2, while there is a fluid-fluid interface of gas and oil between Ω_1 and Ω_2. In Figure 5, the fluid is homogenous in Ω_1 and Ω_2, while there is permeability discontinuity in the porous medium between Ω_1 and Ω_2. In Figures 4 and 5, acoustic properties of the fluid-fluid interface and the porous medium discontinuity are compared when the incident wave is a compressional type II wave and the incident angle is changing. In these two figures, the amplitudes of all reflected and transmitted waves are shown. It is observed that the amplitude curves related to fluid-fluid interface are significantly different from those generated by a porous medium discontinuity. The acoustic properties described by these figures help identify the fluid-fluid interface.

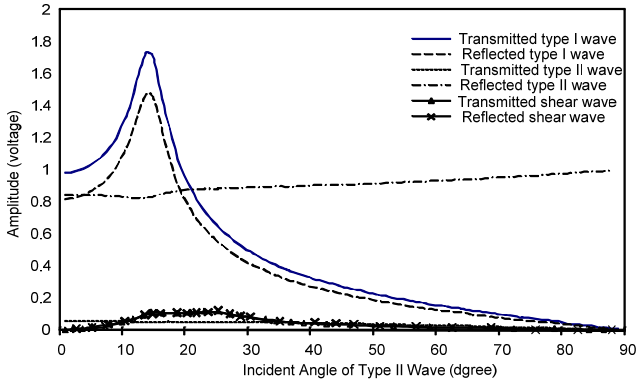

Figure 4. Reflection and transmission amplitudes related to fluid-fluid interface varying with the incident angle.

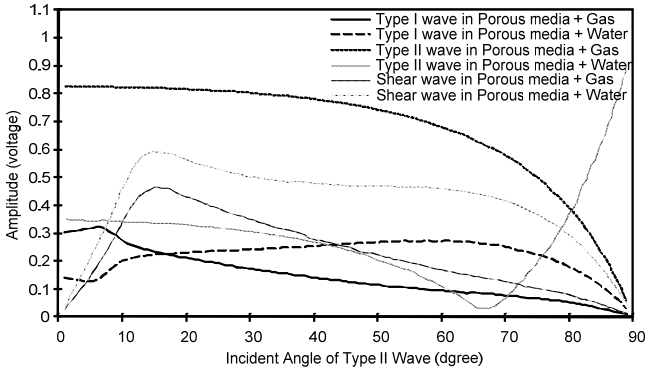

Figure 5. Reflection and transmission amplitudes related to porous medium discontinuity varying with the incident angle.

Similarly, in Figures 6 and 7, the acoustic properties of a fluid-fluid interface and a porous medium discontinuity are compared when the incident wave is a shear wave and its frequency is changing. The X-axis in these figures sweeps the frequency range from 0Hz to over I MHz. This covers a very broad range of frequencies. Once again, it is found that the amplitude curves related to fluid-fluid interface are distinguishable from those related to a porous medium discontinuity. The acoustic properties described by these figures of amplitude vs. frequency help identify the fluid-fluid interface.

Because the physical properties of porous medium and fluids are known, the acoustic characteristics of fluid-fluid interface can be studied in advance. The acoustic characteristics of an unknown interface are investigated with acoustic methods, and compared with those of the fluid-fluid interface in order to determine whether it is a fluid-fluid interface.

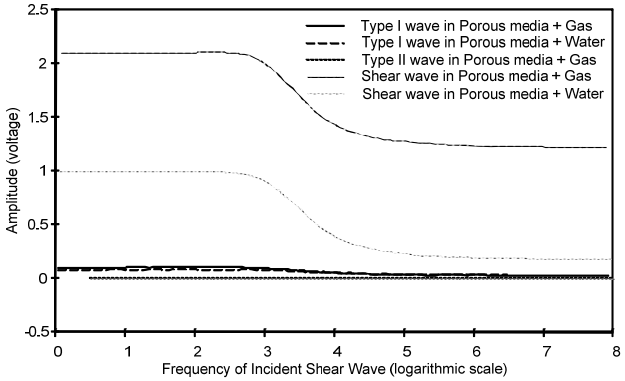

Figure 6. Reflection and transmission amplitudes related to fluid-fluid interface varying with the incident frequency.

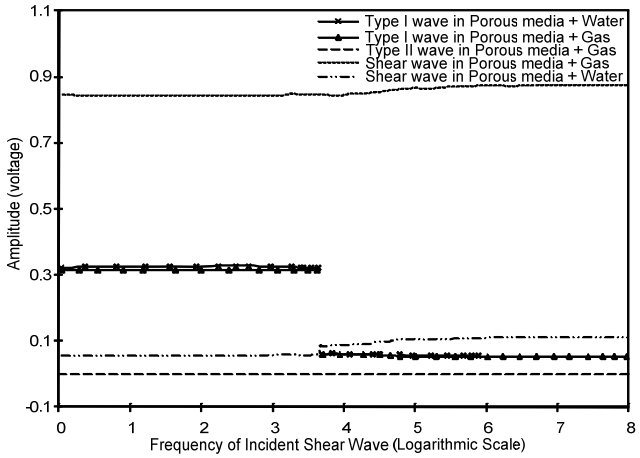

Figure 7. Reflection and transmission amplitudes related to porous medium varying with the incident frequency.

4. Locating the interface

When a fluid-fluid interface in porous medium is identified, it can be located by using reflected waves or transmitted waves. Here, the methodology for determining the location of both linear and curved interfaces is presented.

4.1. Proposed approach to locate a vertical fluid-fluid interface

A vertical line fluid-fluid interface is an idealized and simplified example of this problem. It is assumed that the interface is parallel to the walls of the well, as shown in Figure 8.

When transmitted waves are used to locate the interface, the time of flight of the wave is measured as it is emitted by the transducer in one well and received by the second transducer at the second well. Based on this description, Equation 13 is constructed, in which the time of flight t, the velocities of wave in porous media v_1, v_2, the distance of two wells d are known, while the position of the interface x is the unknown. When this equation is solved, the distance between the well and the interface is obtained. Distance d can be calculated with the similar method when the reflected wave is used:

$$\frac{(d-x)}{v_1}+\frac{x}{v_2}=t \tag{13}$$

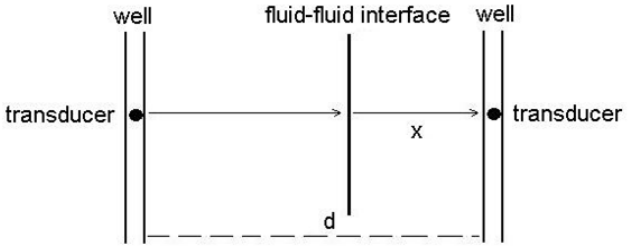

Figure 8. Determine the flat fluid-fluid interface.

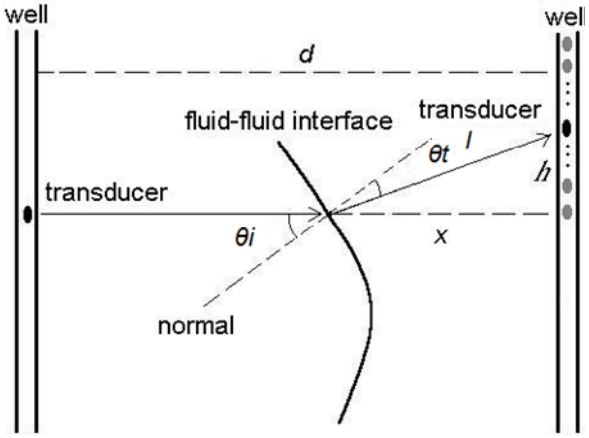

Figure 9. Determine the curved fluid-fluid interface d.

4.2. Proposed approach to locating a curved fluid-fluid interface

In most practical situations, however, the interface is typically curved, see Figure 9. Under these conditions, θ_i and x are unknown variables, while d is measured directly. The value of H can be obtained if we monitor the transmitted wave while moving the receiver along the second well. With geometrical relation of h and x, and with the relationship of the distance, velocities and flight time of waves, a system of Equation (14a) is constructed. If the acoustic properties of the fluid-fluid interface are studied in advance, the relation between θ_t and θ_i can be described with a plot like Figure 3. From Figure 9, l is a function of θ_t, θ_i and x, while θ_t is a function of θ_i, hence l is a function of θ_i and x. Here, the system of equations can be rewritten in the form of Equation (14b), which includes only two unknown variables: x and θ_i. When the system of equations (14b) is solved, both x and θ_i are obtained. When a series of x and θ_i are obtained along the interface, the location and the shape of the front can be determined.

$$\begin{cases} \dfrac{h}{x} = tg(\theta_i - \theta_t) \\ \dfrac{d-x}{v_1} + \dfrac{l}{v_2} = t \end{cases} \tag{14a}$$

$$\begin{cases} f_1(x, \theta_i) = 0 \\ f_2(x, \theta_i) = 0 \end{cases} \tag{14b}$$

5. Conclusions

From the Biot's theory of acoustic wave propagating in fluid saturated porous medium, there are total of six waves generated at a fluid-fluid interface as reflected waves and transmitted waves. These waves can be used to locate the interface and to determine its shape.

The difference of acoustic characteristics is clearly distinguishable between a fluid-fluid interface and discontinuity of porous medium. This can be used to identify a fluid-fluid interface from discontinuities of porous medium. The location and shape of a fluid-fluid interface can be measured with reflected or transmitted waves.

The method presented in this paper has a great potential to support development of an acoustic wave system for monitoring the fluid-fluid interface in reservoirs under CO_2 flooding conditions.

List of Symbols

U = Averaged displacement vector of the solid part of the medium;

U_f = Averaged displacement vector of the fluid part of the medium;

W = Averaged relative fluid displacement per unit volume of bulk material;

φ = Porosity of the solid;

η = Shear modulus of the bulk material, considered to be equal to the shear modulus of the solid matrix;

τ_{zz}, τ_{xz} = Elements of total stress tensor matrix;

E_{mn} = Reflection or transmission coefficient;

K_s = Bulk modulus of the solid grain;

K_f = Bulk modulus of the saturant fluid;

K_m = Bulk modulus of the solid matrix;

K_c = Bulk modulus of the saturated solid;

λ_c = Lamé constant of the saturated solid;

ρ_s = Mass density of the solid grains;

ρ_f = Mass density of the fluid;

ρ = Mass density of the bulk material;

g = Mass coupling coefficients between the solid and fluid phases;

b = Viscous coupling coefficients between the solid and fluid phases;

S = Structure factor;

μ = Fluid viscosity;

k = Solid (rock) permeability;

p = Fluid pressure;

q = Wave propagation index;

ω = Phase velocity of the acoustic wave;

θ = Wave's angle from the normal;

N = Complex wave vector;

C = Concentration of fluid;

v = Local fluid velocity;

D = $K_s K_f (K_s - K_m)/[K_f (K_s - K_m) + K_s \varphi (K_s - K_f)]$;

M = $K_s^2 K_f/[K_f (K_s - K_m) + K_s \varphi (K_s - K_f)]$;

H_c = $\lambda_c + 2\mu$.

References

Albert, D.G. (1993). A Comparison between Wave Propagation in Water-saturated and Air-saturated Porous Materials, *J. Appl. Phys.*, 73(1), 28-36.

Attenborough, K. (1987). On the Acoustic Slow Wave in Air-filled Granular Media, *J. Acoust. Soc. Am.*, 81(1), 93-102.

Attenborough, K. (1993). Models for the Acoustical Properties of Air-saturated Granular Media, Acta Acustica.

Benson, R.D. and Davis, T.L. (2000). Time-Lapse Seismic Monitoring and Dynamic Reservoir Characterization, Central Vacuum Unit, Lea County, New Mexico, *SPE Reservoir Evaluation & Engineering*, 3(1), 88-97, doi:10.2118/60890-PA.

Bear, J. (1972). *Dynamics of Fluids in Porous Media,* New York: American Elsevier Pub. Co.

Deresiewicz, H. (1960). The Effect of Boundaries on Wave Propagation in a Liquid-filled Porous Solid: I. Reflection of Plane Waves at a Free Plane Boundary (Non-dissipative Case), *Bulletin of the Seismological Society of America*, 50(4), 595-625.

Deresiewicz, H., and Rice, J.T. (1962). The Effect of Boundaries on Wave Propagation in a Liquid-filled Porous Solid: III. Reflection of Plane Waves at a Free Plane Boundary (General Case), *Bulletin of the Seismological Society of America*, 52(3), 595-625.

Deresiewicz, H., and Rice, J.T. (1964). The Effect of Boundaries on Wave Propagation in a Liquid-filled Porous Solid: V. Transmission across a Plane Interface, *Bulletin of the Seismological Society of America*, 54(1), 409-416.

Berryman, J.G. (1980). Confirmation of Biot's Theory, *Appl. Phys. Lett.*, 37(4), 382, doi:10.1063/1.91951.

Biot, M.A. (1956). Theory of Propagation of Elastic Waves in a Fluid-Saturated Porous Solid. I. Low-Frequency Range, *J. Acoust. Soc. Am.,* 28(2), 168-178, doi:10.1121/1.1908239.

Biot, M.A. (1956). Theory of Propagation of Elastic Waves in a Fluid-Saturated Porous Solid. II. High-Frequency Range, *J. Acoust. Soc. Am.,* 28(2), 179-191.

Biot, M.A. (1962). Mechanics of Deformation and Acoustic Propagation in Porous Media, *J. Appl. Phys.,* 33(4), 1482, doi:10. 1063/ 1.1728759.

Biot, M.A. (1962). Generalized Theory of Acoustic Propagation in Porous Dissipative Media, *J. Acoust. Soc. Am.*, 34(9), 1254, doi:10. 1121/1.1918315.

Bourbie, T., Coussy, O., and Zinszner, B. (1987). *Acoustics of Porous Media*, Gulf Publishing.

Dutta, N.C., and Ode, H. (1983). Seismic Reflections from a Gas-water Contact, *Geophysics*, 48(2), 148, doi:10.1190/1.1441454.

El-Ahmadi Heiba, A. (1985). Porous Media: Fluid Distributions and Transport with Applications to Petroleum Recovery, Ann Arbor, MI: UMI.

Geertsma, J., and Smit, D.C. (1961). Some Aspects of Elastic Wave Propagation in Fluid-saturated Porous Solids, *Geophysic*s, Vol. XX VI, No.2.

Harris, C.M. (1991). *Handbook of Acoustical Measurements and Noise Control*, New York, McGraw-Hill.

Juprasert, M.S., Haught, M.B., and Schoell, M. (1999). Prediction of Steamflood Performance Using Carbon Isotope Signatures of CO2, presented at SPE Western Regional Meeting, 26-27, Anchorage, Alaska.

Pettigrew, M.J., Taylor, C.E., and Subash, N. (1995). Flow-induced Vibration Specifications for Steam Generators and Liquid Heat Exchangers.

Plona, T.J. (1980). Observation of a Second Bulk Compressional Wave in a Porous Medium at Ultrasonic Frequencies, *Appl. Phys. Lett.*, 36(4), 259-261, doi:10.1063/1.91445.

Ruhovets, N. (1995). Quantitative Monitoring of Gasflooding in Oil-Bearing Reservoirs by Use of a Pulsed Neutron Tool, *SPE Formation Evaluation*, 10(4), 255-258, doi:10.2118/21411-PA.

Santos, J.E., Corbero, J.M., Ravazzoli, C.L., and Hensley, J.L. (1992). Reflection and Transmission Coefficients in Fluid-saturated Porous Media, *J. Acoust. Soc. Am.,* 91(4), 1911-1923, doi:10.1121/1.4 03702.

Scheidegger, A.E. (1974). *The physics of flow through porous media*, Third Edition, University of Toronto Press.

Thomson, W.T. (1981). *Theory of Vibration with Applications*, Prentice-Hall, Inc.

Wu, K.Y., Xue, Q., and Adler, L. (1990). Reflection and Transmission of Elastic Waves from a Fluid-saturated Porous Solid Boundary, *J. Acoust. Soc. Am.,* 87(6), 2349-2358, doi:10.1121/1.399081.